Bioconjugate Chemistry

pubs.acs.org/bc

Article

Arylethynyltrifluoroborate Dienophiles for on Demand Activation of IEDDA Reactions

Zbigniew Zawada,[#] Zijian Guo,[#] Bruno L. Oliveira, Claudio D. Navo, He Li, Pedro M. S. D. Cal, Francisco Corzana, Gonzalo Jiménez-Osés,* and Gonçalo J. L. Bernardes*

Cite This: *Bioconjugate Chem.* 2021, 32, 1812−1822

Read Online

ACCESS | Metrics & More | Article Recommendations | Supporting Information

ABSTRACT: Strained alkenes and alkynes are the predominant dienophiles used in inverse electron demand Diels−Alder (IEDDA) reactions. However, their instability, cross-reactivity, and accessibility are problematic. Unstrained dienophiles, although physiologically stable and synthetically accessible, react with tetrazines significantly slower relative to strained variants. Here we report the development of potassium arylethynyltrifluoroborates as unstrained dienophiles for fast, chemically triggered IEDDA reactions. By varying the substituents on the tetrazine (e.g., pyridyl- to benzyl-substituents), cycloaddition kinetics can vary from fast (k_2 = 21 M^{-1} s^{-1}) to no reaction with an alkyne-BF_3 dienophile. The reported system was applied to protein labeling both in the test tube and fixed cells and even enabled mutually orthogonal labeling of two distinct proteins.

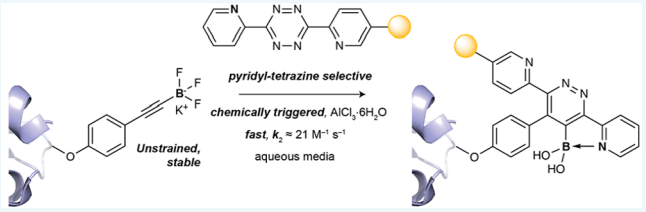

INTRODUCTION

Electron-deficient tetrazines were first reported to react with unsaturated compounds in 1959 by Carboni and Lindsey,[1] but it was not until 2008 that Fox and co-workers re-engineered the inverse electron demand Diels−Alder (IEDDA) reaction between tetrazines and *trans*-cyclooctenes (TCO) for bioorthogonal applications (Figure 1).[2] Since then, efforts have focused on the development of dienophiles with superior reactivity.[3−8] Strained dienophiles are the predominant reactive handles for IEDDA reactions because of their exceptionally fast kinetics (up to 3 × 10^6 M^{-1} s^{-1}; Figure 1a).[3] However, their instability, bulkiness, potential cross-reactivity with biological nucleophiles, and complex synthesis restrict their application.[9,10] Conversely, smaller, unstrained alkenes are synthetically accessible and highly stable under biological conditions but react significantly slower with tetrazines (k_2 ≈ 10^{-3}−10^{-2} M^{-1} s^{-1}; Figure 1b).[11−14] The recently reported vinylboronic acid dienophile, unlike the above-mentioned unstrained alkenes, has satisfactory kinetics (k_2 = 27 M^{-1} s^{-1}), is easily synthesized, and is relatively stable (Figure 1c).[15−17] Development of new unstrained dienophiles remains of interest, particularly if they offer the possibility of orthogonal, consecutive IEDDA reactions. Furthermore, the use of chemical triggers for temporal controllable initiation of the reaction remains elusive. Herein we describe the use of potassium arylethynyltrifluoroborates as stable, unstrained dienophiles for selective and fast IEDDA reactions (Figure 1d). The reaction between bioorthogonal arylethynyltrifluoroborate and dipyridyl tetrazine can be triggered in a temporal-controlled manner by chemical additives. Notably, the alkyne-BF_3 handle only reacts with pyridyl-substituted tetrazines and not with non-*N*-heterocyclic tetrazines. The utility of the reported reaction is demonstrated for protein modification and mutually orthogonal labeling of two proteins that contain either the alkyne-BF_3 handle or a norbornene moiety with a pyridyl- and benzyl-tetrazine, respectively.

Arylethynyltrifluoroborate tetraethylammonium salts undergo reaction with tetrazines in organic solvents (e.g., CH_2Cl_2) in the presence of trimethylsilyl chloride (TMSCl).[18] Despite its excellent reactivity, the use of arylethynyltrifluoroborates as dienophiles for IEDDA ligation has not been tried because of the high reactivity of TMSCl with many biological functional groups as well as TMSCl water incompatibility. Potassium trifluoroborate is a convenient functional group in organic chemistry, in particularly for Suzuki−Miyaura coupling reactions[19] because it is moisture and air stable and inert to strong oxidative conditions.[20] Besides, trifluoroborates are most often solids that are soluble in aqueous media, which makes them easy to handle and store. With this in mind we decided to investigate the potential of arylethynyltrifluoroborates in IEDDA bioorthogonal reactions with tetrazines.

RESULTS AND DISCUSSION

To begin, we focused on engineering the reaction of arylethynyltrifluoroborate with tetrazines in aqueous con-

Received: May 24, 2021
Revised: July 2, 2021
Published: July 15, 2021

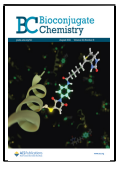

https://doi.org/10.1021/acs.bioconjchem.1c00276
Bioconjugate Chem. 2021, 32, 1812−1822

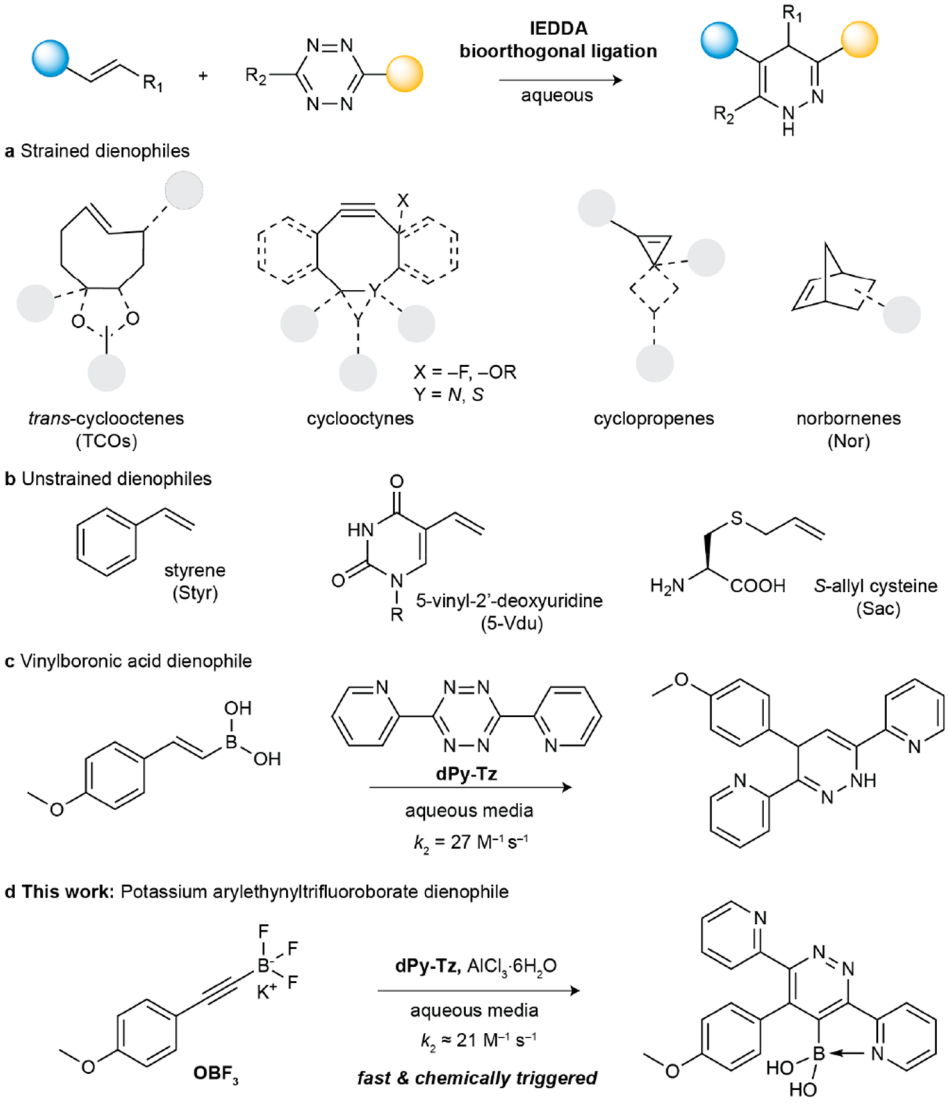

Figure 1. IEDDA reaction between a dienophile and a tetrazine. (a) Strained and (b) unstrained dienophiles as tetrazine coupling partners in IEDDA reactions. (c) Reaction between vinylboronic acid and a dipyridyl tetrazine. (d) Chemically triggered, fast and selective IEDDA reaction between potassium arylethynyltrifluoroborates and pyridyl tetrazines. Py = pyridyl.

ditions (Figure 2). The reaction was performed in a mixture of 40% MeOH in phosphate-buffered saline (PBS) pH 7.4 (*v*/*v*) with potassium phenylethynyltrifluoroborate (**HBF$_3$**) and dipyridyl tetrazine (**dPy-Tz**) as model substrates. Reaction progression was monitored by decay of absorption of **dPy-Tz** at 530 nm. **dPy-Tz** remained stable for 90 min at 30 °C and addition of **HBF$_3$** did not lead to **dPy-Tz** consumption, which suggests a lack of reactivity between potassium arylethynyltrifluoroborate and tetrazine in the absence of chemical triggers. We therefore focused on screening a range of water-compatible additives (KCl, $MgCl_2$, $InCl_3$, $ZnCl_2$, and $AlCl_3{\cdot}6H_2O$) that might trigger the reaction because TMSCl and $BF_3{\cdot}OEt_2$[21−23] were not compatible with aqueous conditions (unstable). Addition of KCl and $MgCl_2$ did not trigger the reaction. Addition of $InCl_3$ or $ZnCl_2$ led to decay of tetrazine absorbance both in the presence and absence of **HBF$_3$**, possibly as a result of coordination of the metal to the tetrazine derivative. Surprisingly, when $AlCl_3{\cdot}6H_2O$ was tested, very fast consumption of **dPy-Tz** was observed (Figure 2d). With $AlCl_3{\cdot}6H_2O$ the reaction is complete in less than 10 min. Importantly, control experiments either in the absence of $AlCl_3{\cdot}6H_2O$ or **HBF$_3$** showed no consumption of **dPy-Tz**. These data demonstrate the potential of inducing fast IEDDA reaction between arylethynyltrifluoroborate dienophiles with tetrazine triggered by $AlCl_3{\cdot}6H_2O$ under aqueous conditions.

Inspired by these results, we investigated various structural motifs that may impact the kinetics of the Al^{3+}-triggered IEDDA reaction. Electronic effects are known to play a key role in the reactivity of dienophiles.[24] Due to the poor stability of some potassium trifluoroborate species in aqueous media,[25] only potassium arylethynyltrifluoroborate derivatives **HBF$_3$**, **OBF$_3$**, and **FBF$_3$** were tested (Figure 3a, entries 1−3). Our screening data indicate that electron-donating **OBF$_3$** reacted the fastest ($k_2 \approx 4.9\ M^{-1}\ s^{-1}$) followed by **HBF$_3$** ($k_2 \approx 1.8\ M^{-1}\ s^{-1}$) with a fixed amount of $AlCl_3{\cdot}6H_2O$ (5 equiv). The slowest rate observed was for **FBF$_3$** as a result of π-electron withdrawal by fluorine atoms ($k_2 \approx 0.9\ M^{-1}\ s^{-1}$). These results are in accordance with the general principles of IEDDA reactions that electron-rich dienophiles feature a smaller $HOMO_{dienophile}$-$LUMO_{diene}$ energy gap and thus accelerate the reaction.[24]

https://doi.org/10.1021/acs.bioconjchem.1c00276
Bioconjugate Chem. 2021, 32, 1812−1822

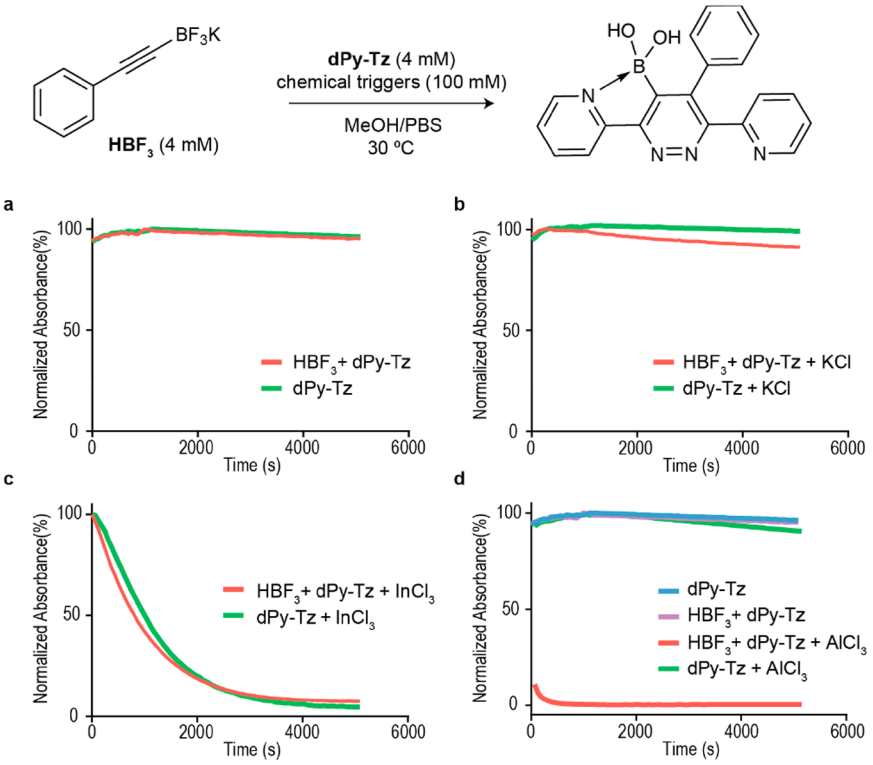

Figure 2. Aqueous reaction between HBF_3 and dPy-Tz. (a–d) Screening of additives. Reaction conditions: **dPy-Tz** (4 mM), **HBF_3** (4 mM), and additives (100 mM) in MeOH/PBS (40%). Monitored at 530 nm at 30 °C. See the Supporting Information (Figure S4) for results with $MgCl_2$ and $ZnCl_2$ as additives.

Arylethynyltrifluoroborates with different lipophilic counterions were also examined (Figure 3a, entries 4 and 5). By replacing potassium with a tetraethylammonium or tetrabutylammonium cation the reaction was slower. Overall, the data show potassium **OBF_3** is the most suitable unstrained dienophile for IEDDA reactions with **dPy-Tz**.

Next, we explored the reactivity of potassium arylethynyltrifluoroborate toward different tetrazines. Interestingly, we observed that non-pyridyl-containing tetrazines displayed exceedingly low reactivity toward **OBF_3** (Figure 3c), whereas **PyMe-Tz** (Figure 3b), which contains only one appended pyridyl group, showed decreased reactivity in the presence of Al^{3+}($k_2 \approx 0.2\ M^{-1}\ s^{-1}$ for **PyMe-Tz** versus $k_2 \approx 4.9\ M^{-1}\ s^{-1}$ for **dPy-Tz** under the same conditions). This reactivity trend is consistent with the boron–nitrogen-directed mechanism (responsible also for the high regioselectivity of the reaction with **PyMe-Tz**) previously reported for vinylboronic acid dienophiles.[15,18] We further confirmed this notion for arylethynyltrifluoroborate through DFT calculations (Figure 3d). Once $AlCl_3{\cdot}6H_2O$ is introduced into the system, it instantaneously defluorinates the alkynyltrifluoroborate to yield the corresponding difluoroalkynylborane *in situ* in a very thermodynamically favored way (Figure S2). The resulting difluoroalkynylborane then forms an alkynyltetrazine-adduct mediated by a strong boron–nitrogen bond. Subsequent rate-limiting [4 + 2] cycloaddition proceeds very fast due to the small energy barrier ($\Delta G^{\ddagger} \approx 13$ kcal mol^{-1}). When the same difluoroalkynylborane reacts with non-pyridyne-containing tetrazines, the energy barrier for cycloaddition significantly increases ($\Delta G^{\ddagger} \approx 35$ kcal mol^{-1}, Table S1) similarly to the very slow reaction predicted between nondefluorinated alkynyltrifluoroborates and pyridyl-tetrazines, which explains the reaction selectivity toward different tetrazines. The reaction rate is comparable to the recently reported vinylboronic acid dienophile.[17] Thus, the reaction between optimal ethynyltrifluoroborate (**OBF_3**) and tetrazine (**dPy-Tz**) afforded IEDDA cycloaddition product in 96% yield (Figure 3f) after 15 min.

With these preliminary results in hand, we decided to study the kinetics of the model reaction (with **dPy-Tz** and **HBF_3**) in more detail. First, we measured the partial reaction order of reactants by the initial rates method. As expected, they were determined as 1.0 for **dPy-Tz** and 1.0 for **HBF_3**. However, this method was not suitable for calculating the partial reaction order for $AlCl_3{\cdot}6H_2O$. We analyzed this phenomenon further and found that the reaction rate is sensitive to both ionic strength and pH, which are both affected by change of concentration of $AlCl_3{\cdot}6H_2O$. Thus, the 12.5-fold increase of its concentration (from 20 mM to 250 mM) led to 2.2-fold increase of the reaction rate, which would formally provide partial reaction order of 0.3. We attribute the small relative increase of reaction rate (in comparison with the increase of the concentration) to the increase in ionic strength because addition of LiCl to the reaction solution can increase the reaction rate over 3-times (vide infra, Table 1). The concomitant decrease of pH contributes to reaction acceleration as well; the equivalent change of solution pH (from 3.58 to 2.84) increases the reaction rate 1.2-fold (Figure 4). Due to the low solubility of reaction components in the reaction solution, we did not manage to measure both influences of $AlCl_3{\cdot}6H_2O$ in isolation. Nevertheless, we concluded that the partial reaction order of $AlCl_3{\cdot}6H_2O$ is 0.

The influence of solution pH is more complex (Figure 4a,b). The reaction is slow over pH 5, which can be explained in part

https://doi.org/10.1021/acs.bioconjchem.1c00276
Bioconjugate Chem. 2021, 32, 1812–1822

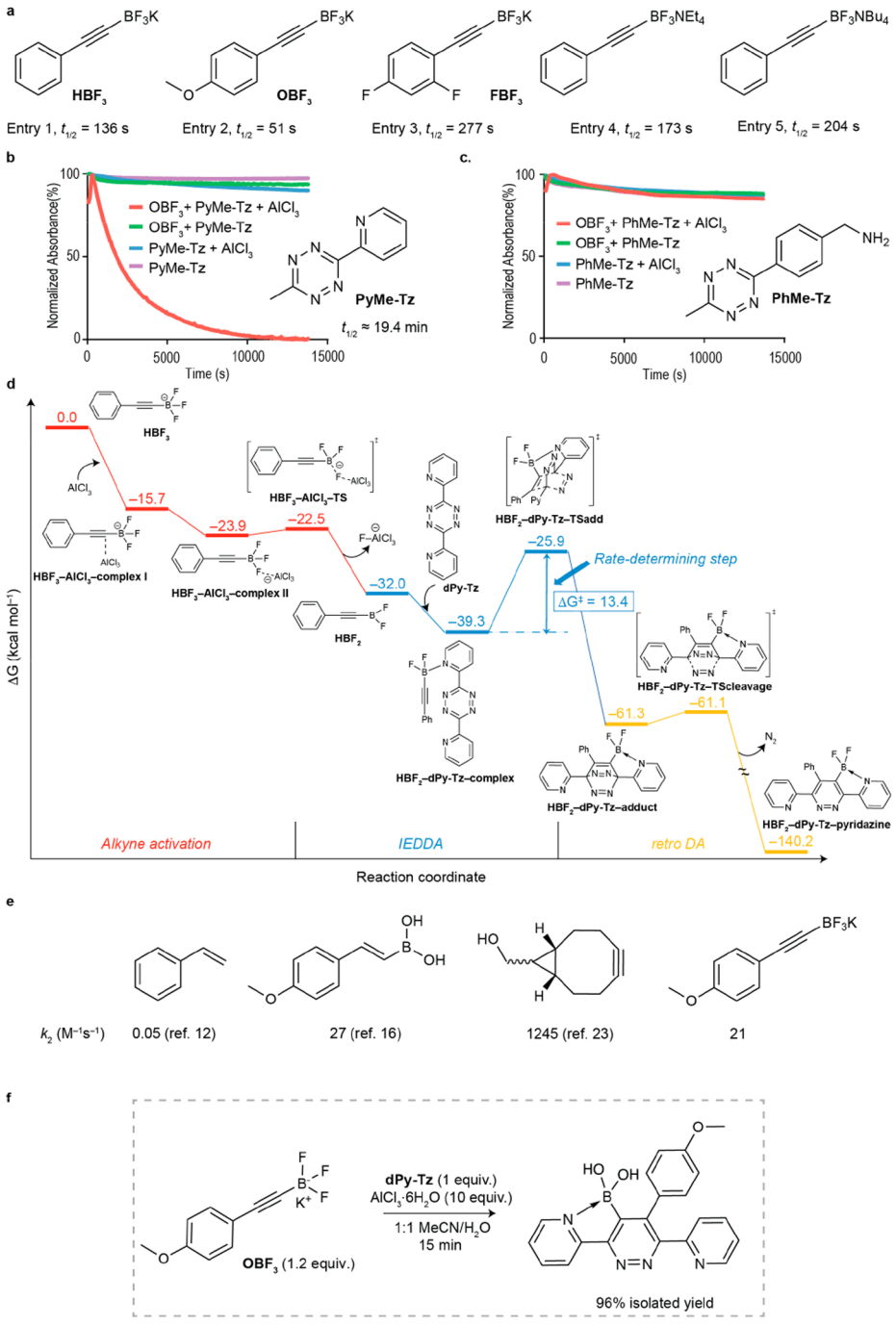

Figure 3. Kinetic and computational studies. (a) Half-life of the reaction between arylethynyltrifluoroborate salts (4 mM), **dPy-Tz** (4 mM), and $AlCl_3 \cdot 6H_2O$ (20 mM) in a mixture of 40% MeOH/PBS followed at 530 nm at 30 °C. (b and c) Absorbance decay upon reaction of $\mathbf{OBF_3}$ with different tetrazines. (d) Complete energy profile for the reaction of arylethynyltrifluoroborate $\mathbf{HBF_3}$ and tetrazine **dPy-Tz** calculated at PCM(H_2O)/M06-2X/6-31+G(d,p) level. The activation (i.e., defluorination, in red), IEDDA reaction (in blue) and retro-DA leading to the final pyridazine (in yellow) are all fast and thermodynamically very favored. Activation ($\Delta G^{\ddagger}$) and reaction energies (ΔG) are in kcal mol^{-1}. (e) Comparison of reported[26] second-order rate constants. (f) Reaction between optimal ethynyltrifluoroborate $\mathbf{OBF_3}$ (24 mM) and tetrazine **dPy-Tz** (20 mM) triggered by $AlCl_3 \cdot 6H_2O$.

by formation of insoluble hydroxide complexes $Al(OH)_n^{3-n}$. The reaction is accelerated significantly below pH 2. In between, the reaction rate increases with decreasing pH. The reaction acceleration in acidic conditions can be explained by partial protonation of the pyridine moieties of **dPy-Tz**. The pyridinium cation formed (**dPyH$^+$-TzH**) is more electron withdrawing relative to pyridine, so it lowers the energy of the tetrazine LUMO, which in turn decreases the HOMO−LUMO energy gap of the IEDDA reaction (the rate-limiting step). This finding is in good agreement with our DFT calculations that show that protonation decreases the activation barrier of the rate-limiting step by 2.5 kcal mol^{-1} thus accelerating the reaction nearly 70-fold at room temperature (Figure 4b). However, complete protonation of

https://doi.org/10.1021/acs.bioconjchem.1c00276
Bioconjugate Chem. 2021, 32, 1812−1822

Table 1. Reaction Rate Constants of Click Reactions with dPy-Tz in Various Conditions

dienophile	solvent[a]	LiCl (M)	$AlCl_3 \cdot 6H_2O$ (mM)	T (°C)	k_2 (M^{-1} s^{-1})
HBF_3	H_2O		250	30.0	4.1
HBF_3	PBS		250	30.3	4.3
HBF_3	H_2O	3	250	30.0	13.0
OBF_3	H_2O	3	250	30.5	21.1
HBF_3	H_2O			30.2	NR
HBF_3	H_2O	3		30.2	NR
	H_2O	3	250	30.0	NR
1[b]	H_2O		250	30.7	1.7
1[b]	H_2O	3	250	30.7	2.3
2	H_2O			30.2	0.07
2	H_2O		250	30.2	0.09
2	H_2O	3		30.2	0.11
2	H_2O	3	250	30.0	0.15

[a]H_2O and PBS stand for: 59.5% H_2O, 36% MeOH, and 4.5% NMP and 49% PBS, 10.5% H_2O, 36% MeOH, and 4.5% NMP, respectively. [b]Estimated reaction rate of *endo*- and *exo*- isomers of 5-norbornen-2-ol mixture. NR, no reaction.

both pyridines (**$dPyH_2^{2+}$-TzH**) precludes coordination to the BF_2 group of the reacting alkyne and increases the cycloaddition activation barrier dramatically by nearly 20 kcal mol^{-1}. An apparent kinetic rate constant (k_{obs}) was estimated from the individual theoretical constants of each reaction between **HBF_3** and **dPy-Tz** in different protonation states (k), and the dissociation constants for each species (K_a; Figure 4b and eq 1 in the SI). In qualitative agreement with experimental measurements, this calculated k_{obs} shows a large pH-dependency and supports the significant acceleration observed under highly acidic conditions.

We were also interested in the influence of ionic strength on the reaction rate. From all tested neutral salts (LiCl, NaCl, KCl, and CsCl) only LiCl was soluble enough in the reaction mixture. As can be seen from Table 1, 3 M LiCl speeded up the reaction 3.2-times (4.1 M^{-1} s^{-1} vs 13.0 M^{-1} s^{-1}), which is in agreement with the reported influence of LiCl on Diels–Alder reactions.[27] The reaction rate was increased further to 21.1 M^{-1} s^{-1} by replacing **HBF_3** with **OBF_3**, which is consistent with our preliminary measurements.

For comparison, we measured the kinetics between **dPy-Tz** and two norbornene derivatives (Figure 5): 5-norbornen-2-ol (**1**) and 5-norbornene-2-endo,3-exodicarboxylic acid (**2**). We measured their sensitivity to LiCl and $AlCl_3 \cdot 6H_2O$ under identical conditions (Table 1). Both norbornene derivatives have their highest reaction rate in the presence of both additives (LiCl and $AlCl_3 \cdot 6H_2O$, Table 1). Each additive increases the reaction rate; however, LiCl has greater impact relative to $AlCl_3 \cdot 6H_2O$. This might be explained by higher ionic strength of LiCl (3 M) versus $AlCl_3 \cdot 6H_2O$ (0.25 M). The addition of LiCl speeds up both click reactions; however, the reaction rate with **HBF_3** is increased 3.2-times, whereas reaction with norbornene **2** is increased only 2.1-times. Reaction with norbornene proceeds in the absence of Al^{3+}, which is not the case for the ethynyltrifluoroborate based click reaction—the reaction is triggered by Al^{3+}.

Interestingly, although it has been reported that unsubstituted norbornene reacts faster[28] than any mono- or disubstituted derivative and that electron-withdrawing groups further slow down the reaction,[28] reported reaction rate of unsubstituted norbornene with **dPy-Tz** in methanol has the same value[28] (0.15 M^{-1} s^{-1}) as our reaction of disubstituted norbornene. This can be attributed to the presence of additives and water which accelerates[29] Diels–Alder reactions. Nevertheless, even monosubstituted norbornene **1** with an electron-donating group (which is almost as reactive as unsubstituted norbornene[28]) reacts with **dPy-Tz** approximately 9-times slower than trifluoroborate **OBF_3**.

Next, we expanded the scope of the reaction and applied it to protein labeling. As proof of concept, a tetrazine (**caa-dPy-Tz**) or an arylethynyltrifluoroborate (**caa-OBF_3**) moiety was installed into a linker that featured a carbonylacrylic acid (caa) handle for cysteine-selective bioconjugation (Figure 6a; see pages S43–S47 in the SI for synthetic details).[30,31] Since trifluoroborates can be principally hydrolyzed, we first assessed the hydrolytic stability of **caa-OBF_3** and its stability toward thiols (glutathione; see Chapter 4 in the SI). Less than 1% of **caa-OBF_3** decomposed after 3 days in 40% D_2O/DMSO at 37 °C. Further treatment at room temperature (18 days) left 90% of **caa-OBF_3** intact. The sample was further treated with reduced glutathione (5 equiv., 25 mM) for another 30 h at 37 °C. As expected, the caa handle reacted smoothly with the thiol group of glutathione to afford a glutathione adduct with **caa-OBF_3** after 10 min. Nevertheless, only ∼10% of the trifluoroborate moiety of **caa-OBF_3** decomposed in the presence of the thiol after 30 h. After both stability tests, the sample was further tested for the ability to react with **dPy-Tz**. As expected, **caa-OBF_3** afforded the click product in the presence of Al^{3+} even after 22 days of stability tests. Thus, **caa-OBF_3** is not only stable against hydrolysis in aqueous media but its **OBF_3** moiety is also sufficiently stable against nucleophiles, which makes **caa-OBF_3** suitable for installation on proteins through cysteine conjugation.

Further we tested the reaction on three model proteins: ubiquitin (Ub),[32] the C2A domain of Synaptotagmin-I (C2Am),[33] and anti HER2 nanobody (2RB17C).[34] All proteins were engineered with one surface-exposed cysteine (Figure 6b). We started with the installation of the **caa-OBF_3** dienophile on the proteins for subsequent IEDDA labeling with **dPy-Tz** in the presence of $AlCl_3 \cdot 6H_2O$ as a chemical trigger. Reaction of 2RB17C nanobody with **caa-OBF_3** (5 equiv) afforded desired 2RB17C-**caa-OBF_3** at 25 °C after 1 h. However, three other species with lower masses and an interval of 20 Da were also observed on the mass spectrum. We attributed them to potential defluorination products of BF_3 moiety during LC-MS analysis. The product was dialyzed and then reacted with **dPy-Tz** (100 equiv) in the presence of Al^{3+} (100 equiv). The reaction was complete after 3 h in a pH 4.5 buffered solution at 37 °C (Figure S26). When $AlCl_3 \cdot 6H_2O$ was omitted, no reaction was observed under the same conditions after 5 h. The excess of **dPy-Tz** was necessary to compensate for the much lower concentration of tagged protein (15 μM) relative to the small-molecule reagents used for reaction engineering (4 mM). It is important to mention that the reaction on proteins proceeds smoothly in acidic conditions but not in neutral buffers, which is consistent with our data on small-molecule systems. Thus, IEDDA labeling of protein can be completely temporally controlled: it can be turned on by addition of $AlCl_3 \cdot 6H_2O$ trigger and off by an increase in pH to 7.0–7.4.

Further we tested the IEDDA reaction compatibility with even more acidic conditions on Ub conjugate. We prepared Ub-**caa-OBF_3** by reaction of Ub with **caa-OBF_3** (Figure 6f).

https://doi.org/10.1021/acs.bioconjchem.1c00276
Bioconjugate Chem. 2021, 32, 1812–1822

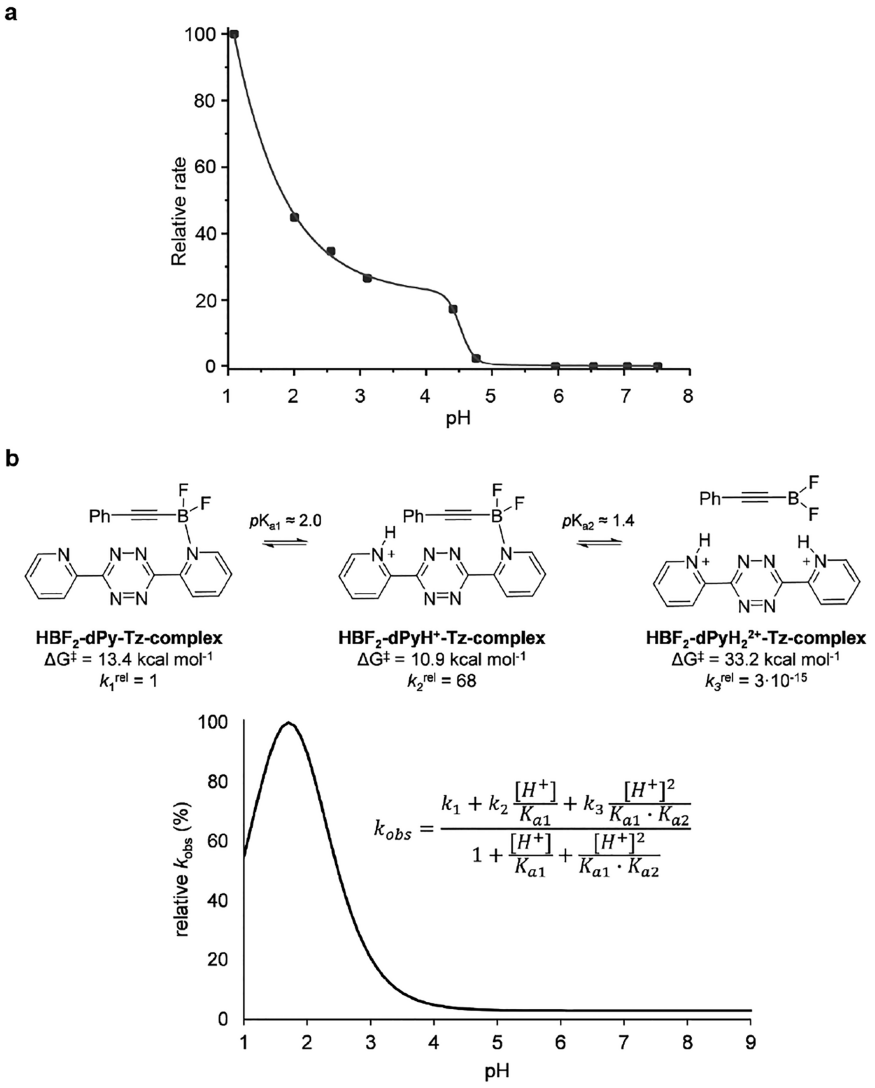

Figure 4. (a) Dependence of relative rate of model reaction between **dPy-Tz** and HBF_3 on pH. (b) Theoretical relative rate constants (k_{obs}) calculated at different pH values for the parallel, competitive reactions of HBF_3 with **dPy-Tz** in different protonation states (**dPy-Tz**: neutral; **dPyH$^+$-Tz**: protonated; **dPyH$_2^{2+}$-Tz**: doubly protonated). The curve was generated using the intrinsic reaction rate constants (k_1, k_2, and k_3) derived from the corresponding calculated activation barriers ($\Delta G^{\ddagger}$), and the equilibrium constants (pK_{a1} = 2.0; pK_{a2} = 1.4) estimated with Marvin 19.19.0, 2019, ChemAxon (http://chemaxon.com).

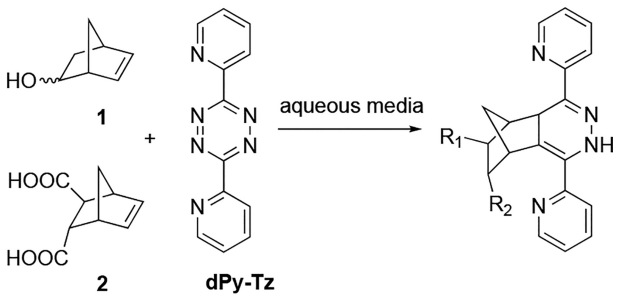

Figure 5. Click reaction between norbornene derivatives (**1** and **2**) and **dPy-Tz** measured under identical conditions as reaction with HBF_3.

The reaction was complete at 25 °C after 2 h and afforded the product (Figure 6g) and again three other species with lower masses with interval of 20 Da (mono-, di-, and tri-dehydrofluorinated species). Upon dialysis, the product was reacted with **dPy-Tz** in the presence of Al^{3+}. At pH 4, the reaction was complete after 30 min at 37 °C and gave a single mass peak corresponding to the desired IEDDA ligation product (Figure 6h). As expected, the reaction was slower at pH 4.7: only 60% of product was formed after 1 h at 37 °C (Figure S23). Under these conditions, boronic acid corresponding to difluoroalkynylborane hydrolysis was observed as well. The formed boronic acid did not react even with 100 equiv of **dPy-Tz**, which suggests that **dPy-Tz** reacted chemoselectively with difluoroalkynylborane. Thus, not only is the IEDDA step compatible with acidic conditions, but consistent with our kinetics measurements, it is also accelerated by lower pH. Under acidic conditions, we have observed slow product formation without Al^{3+} (Figures 7b, lane 2). Since the overall reaction cascade starts by defluorination of the BF_3 moiety promoted by $AlCl_3{\cdot}6H_2O$, we envisioned that acidic conditions could also promote this step. Our DFT calculations supported defluorination of BF_3 under acidic conditions, although with a higher energy barrier

https://doi.org/10.1021/acs.bioconjchem.1c00276
Bioconjugate Chem. 2021, 32, 1812−1822

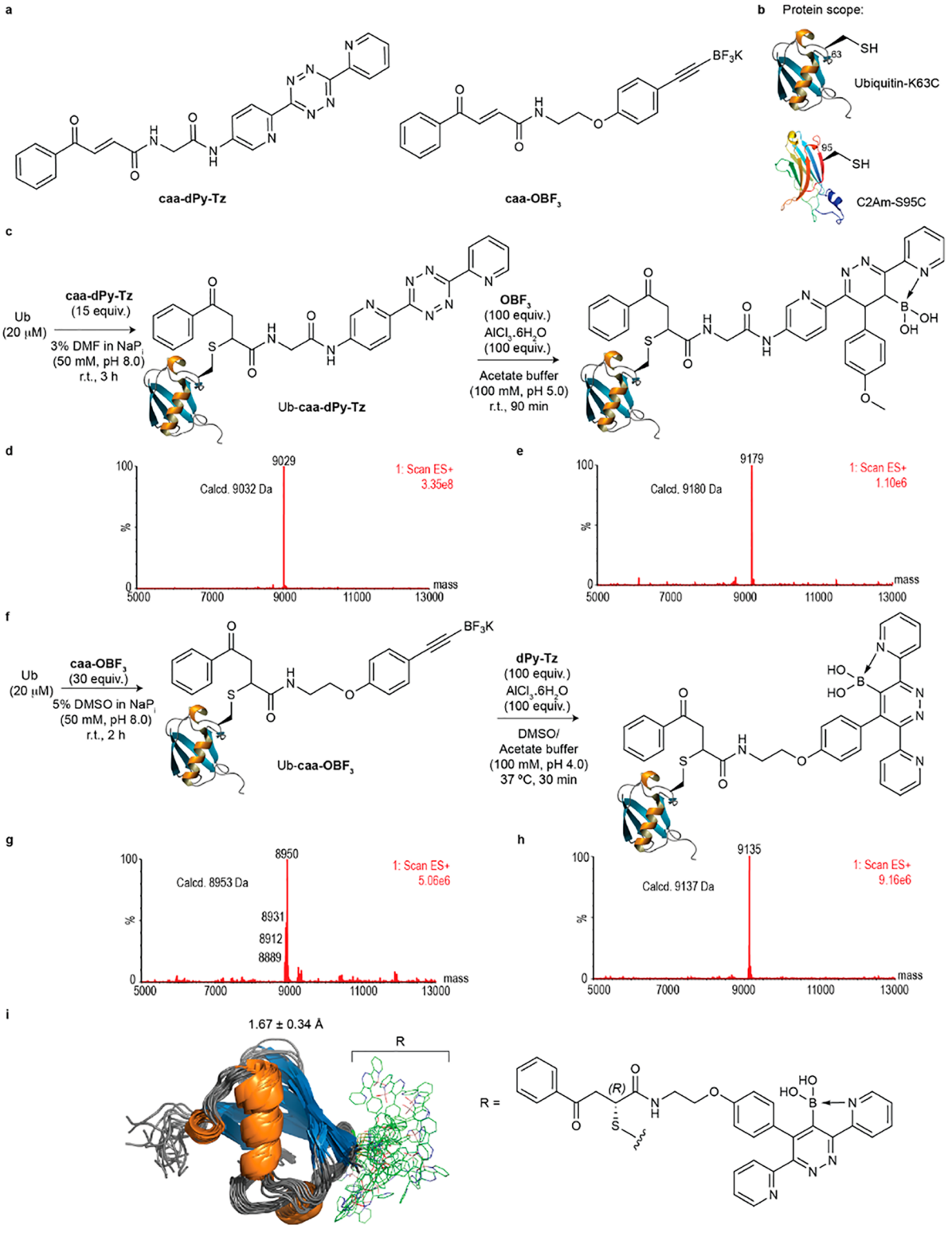

Figure 6. Protein site-selective modification by Al^{3+}-triggered IEDDA reaction. (a) Carbonylacrylic linkers with **OBF_3** or **dPy-Tz**. (b) Protein scaffolds used. (c–e) Installation of **caa-dPy-Tz** on Ub followed by IEDDA reaction with **OBF_3**, and deconvoluted mass spectra of respective products. (f–h) Installation of **caa-OBF_3** on Ub followed by IEDDA reaction with **dPy-Tz**, and deconvoluted mass spectra of respective products. See Chapter 6 in the SI for labeling of C2Am and 2RB17C. (i) Structural ensemble obtained from 0.5 μs MD simulations of the conjugate prepared by reacting Ub-**caa-OBF_3** with **dPy-Tz**. The numbers indicate the rmsd for heavy-atom superimposition of the backbone of the protein relative to the starting structure. DMF = *N*,*N*-dimethylformamide, DMSO = dimethyl sulfoxide.

relative to the Al^{3+}-mediated reaction (Figure S2, SI). This explains the slow overall reaction in acidic conditions in the absence of Al^{3+}. The acceleration of the reaction by acid in the presence of Al^{3+} can be explained by protonation of the

https://doi.org/10.1021/acs.bioconjchem.1c00276
Bioconjugate Chem. 2021, 32, 1812–1822

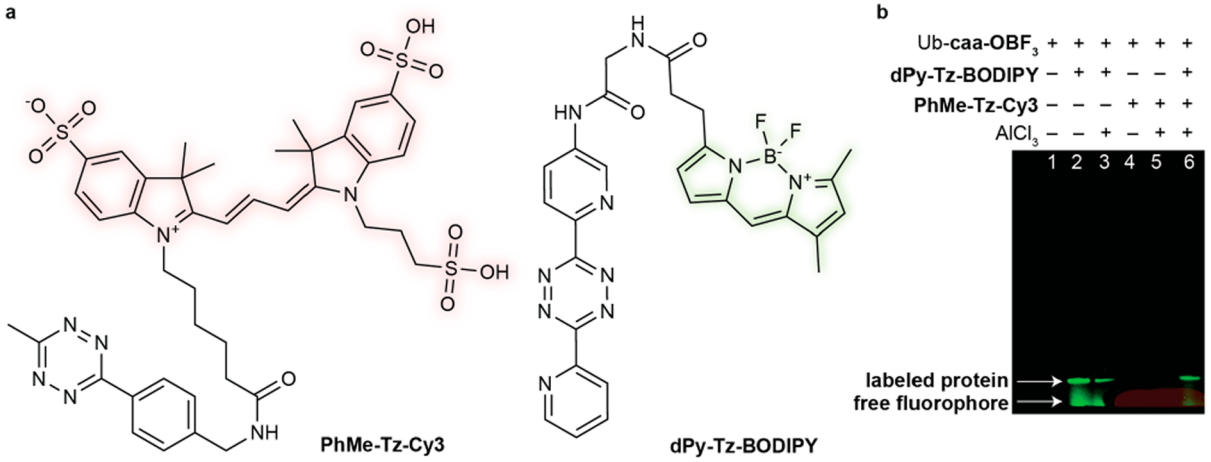

Figure 7. (a) Structures of tetrazine fluorophores. (b) Selective labeling of Ub-**caa-OBF$_3$** with two tetrazine fluorophores as analyzed by SDS-polyacrylamide gel electrophoresis.

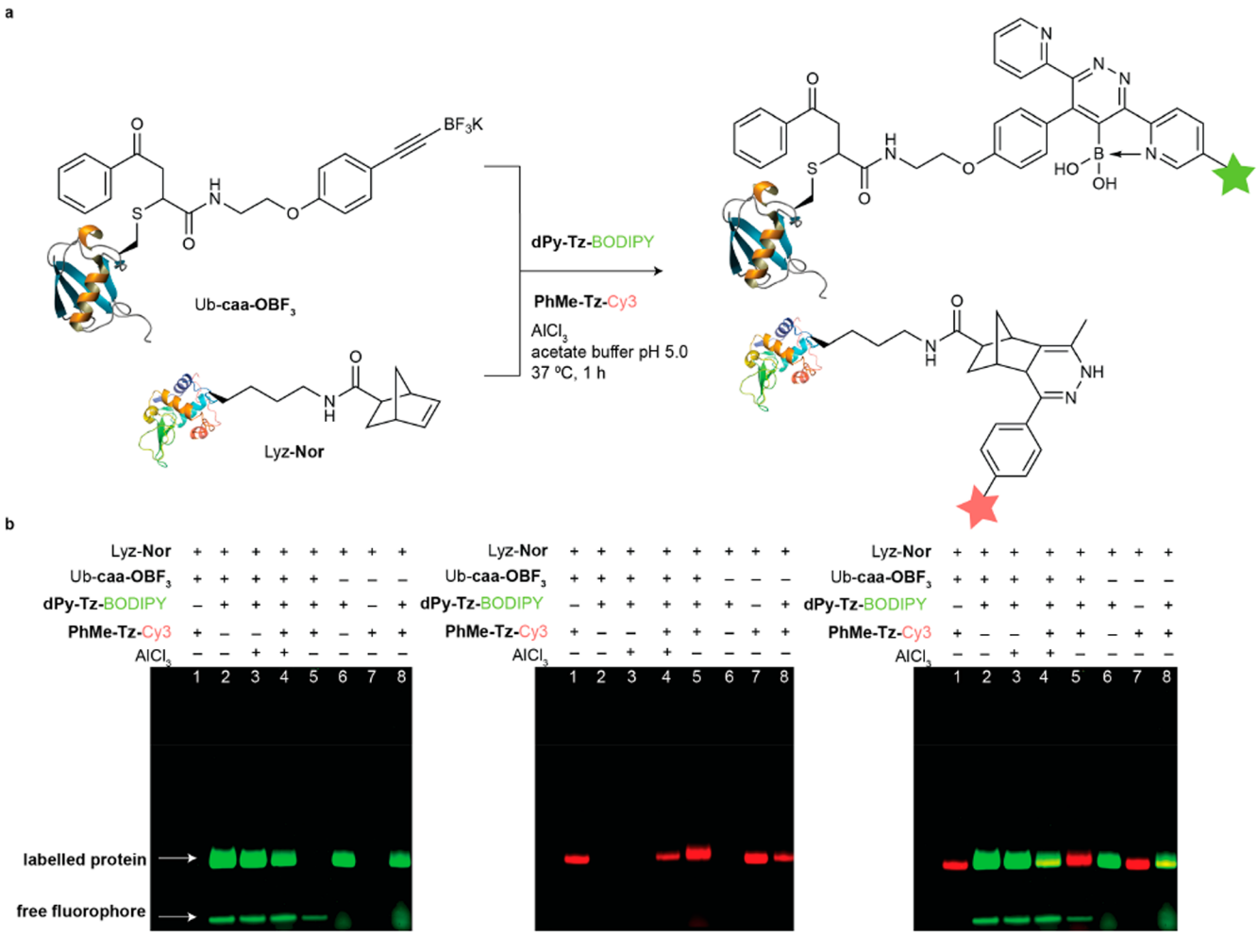

Figure 8. Mutually orthogonal labeling of Lyz-Nor and Ub-caa-BF$_3$ with tetrazine fluorophores **PhMe-Tz-Cy3** and **dPy-Tz-BODIPY**. (a) Representative scheme. (b) SDS−polyacrylamide gel electrophoresis analysis. From left to right: BODIPY channel, Cy3 channel, fluorescence overlap.

pyridine moiety as discussed above. As a result, the overall reaction cascade is fully compatible with acidic buffers, and moreover, it proceeds faster under such conditions.

We explored the possibility of installing **caa-dPy-Tz** instead of **caa-OBF$_3$** on the protein for subsequent IEDDA labeling, however, **caa-dPy-Tz** has limited solubility in aqueous media, which makes this approach less suitable. Nevertheless, complete conversion into desired conjugate Ub-**caa-dPy-Tz** was obtained with **caa-dPy-Tz** (15 equiv) at 25 °C after 3 h, as confirmed by LC-MS analysis (Figure 6c,d). We decided to

https://doi.org/10.1021/acs.bioconjchem.1c00276
Bioconjugate Chem. 2021, 32, 1812−1822

test the combined use of acidic pH and $AlCl_3 \cdot 6H_2O$ to promote a fast IEDDA reaction on protein substrates. After dialysis into acetate buffer (pH 5), Ub-**caa-dPy-Tz** was treated with $\mathbf{OBF_3}$ (100 equiv) in the presence of $AlCl_3 \cdot 6H_2O$ (100 equiv) to give complete conversion into the desired labeled protein after 90 min at 25 °C (Figure 6c,e). IEDDA protein labeling is also possible with less reactive dienophile $\mathbf{HBF_3}$ (4 h at 25 °C; pH 4; Figure S16). In contrast, $\mathbf{FBF_3}$ did not afford any product under similar conditions (4 h at 25 °C; pH 4; data not shown), which is in accordance with our kinetic studies on small molecules. A similar result was observed with **caa-dPy-Tz** installed into C2Am. At pH 4, the reaction with $\mathbf{OBF_3}$ resulted in complete conversion into homogeneous product after 1 h at 37 °C (Figure S20). All results on proteins show that both **caa-**$\mathbf{OBF_3}$ and **caa-dPy-Tz** can be chemically installed on proteins. Subsequent site-selective labeling can be triggered by $AlCl_3 \cdot 6H_2O$. The reaction is fast under acidic conditions but it does not proceed under neutral conditions, which provides an opportunity for full temporal control (on/off) of the reaction. It also offers potential to use two orthogonal IEDDA reactions under different conditions.

MD simulations of the conjugates derived from Ub suggest that the 3D structure of the protein remains unaltered by site-selective introduction of the chemical modifications (Figures 6i and S37), which is required to retain its biological function(s).

Because potassium arylethynyltrifluoroborates reacted with pyridyl tetrazines (**dPy-Tz**) yet remained unreacted in the presence of nonpyridyl tetrazines (e.g., PhMe-Tz), we explored the possibility of selective labeling of Ub-**caa-**$\mathbf{OBF_3}$ by treatment with **dPy-Tz-BODIPY** (Figure 7a) in the presence of **PhMe-Tz-Cy3**. In accordance with experiments on small molecule models, the protein was labeled only by **dPy-Tz-BODIPY** (Figure 7b, lanes 2 and 3 of the gel electrophoresis) but not by **PhMe-Tz-Cy3** (Figure 7b, lanes 4 and 5). Of note is that the reaction with **dPy-Tz-BODIPY** occurs in the absence of Al^{3+}, despite being significantly slower (Figure 7b, lane 2, and S33). This effect is related to the increased reactivity of **dPy-Tz** at acidic pH and the alleged defluorination of BF_3 under acidic conditions as confirmed by DFT calculation and experimental observation (Figure S2).

This unique selectivity inspired us to design new IEDDA pairs for mutually orthogonal labeling of proteins. Recently, the different steric and electronic effects of cyclopropene/TCO and TCO/strained cyclooctyne pairs was explored to develop a multicolor labeling approach by reaction with appropriate tetrazines.[35−37] Similarly, we explored the observed boron−nitrogen-directed selectivity for the mutual labeling of $\mathbf{OBF_3}$- and norbornene (**Nor**)-tagged proteins by simultaneous reaction with pyridyl- and benzyl-substituted tetrazines. We envisioned that if a mixture of lysozyme (Lyz)-**Nor** and Ub-**caa-**$\mathbf{OBF_3}$ is treated with red fluorescent **PhMe-Tz-Cy3** and green fluorescent **dPy-Tz-BODIPY** tetrazines, Lyz-**Nor** would be labeled with **PhMe-Tz-Cy3**, whereas Ub-**caa-**$\mathbf{OBF_3}$ would be labeled with **dPy-Tz-BODIPY**, to result in a red fluorescent Lyz and a green fluorescent Ub, respectively (Figure 8a,b). As expected, **PhMe-Tz-Cy3** reacted with strain-activated Lyz-**Nor** but not with Ub-**caa-**$\mathbf{OBF_3}$ (due to the absence of B−N(Py) interactions) to yield only a red fluorescence band for Lyz (lanes 1 and 7; left and middle panel). Conversely, both proteins reacted with **dPy-Tz-BODIPY** and green fluorescence bands were observed for Lyz-**Nor** and Ub-**caa-**$\mathbf{OBF_3}$ (lanes 2, 3, and 6; left panel). Mixing both fluorescent tetrazines (20-fold excess of less-reactive **PhMe-Tz-Cy3**) with the two proteins led to exclusive formation of red-fluorescent Lyz (lane 5, left and middle panel) as Ub-**caa-**$\mathbf{OBF_3}$ did not react with **PhMe-Tz-Cy3** (Figure 7b, lanes 4 and 5) nor with **dPy-Tz-BODIPY** in the absence of Al^{3+}. However, mixing both fluorescent tetrazines (in equimolar ratio) with the two proteins resulted in the labeling of Lyz-**Nor** with both **PhMe-Tz-Cy3** and **dPy-Tz-BODIPY** (lane 4; compare lane 4 with lanes 1 and 7 of the middle panel). Since Lyz-**Nor** reacted preferably with **dPy-Tz-BODIPY** when both tetrazines were present (lane 6, 7, 8), 20-fold excess of **PhMe-Tz-Cy3** was used to achieve orthogonal labeling of Lyz-**Nor** (lane 5) in the presence of **dPy-Tz-BODIPY**. This experiment suggests that arylethynyltrifluoroborate dienophiles may be used in orthogonal labeling strategies.

Next, we showed the compatibility of the reactants (dienophile and tetrazine) and reaction conditions for labeling experiments in cells. Because of the potentially damaging labeling conditions to live cells, we decided to perform the labeling on fixed SK-BR-3 cells (overexpressing HER2 receptor; Figure 9). First, the cells were incubated (80 min) with 2RB17C-**caa-**$\mathbf{OBF_3}$ (anti HER2 nanobody attached to **caa-**$\mathbf{OBF_3}$, 600 nM). After washing (see Chapter 8 in the SI), the cells were incubated (3 h) with the reaction mixture that contained **dPy-Tz-BODIPY** (300 μM) and $AlCl_3 \cdot 6H_2O$ (5 mM) in acetate buffer (pH 4.5). Then the cells were washed and analyzed by epifluorescent microscopy (Figure 9). The control experiment was performed in the same way except that the nanobody was not used. Fluorescence intensity was higher when using the nanobody relative to control, showing that both proteins (the HER2 receptor and the nanobody) maintained their activity under the reaction conditions. Some fluorescence was detected in the control experiment which is most probably due to unspecific staining by **dPy-Tz-BODIPY** caused by high lipophilicity of the compound. We managed to remove partially the background fluorescence by washing with 50% DMF.[38] Thus, the arylethynyltrifluoroborate dienophile, tetrazine, and the IEDDA conditions we developed are compatible with proteins so they can be used for immunostaining on fixed cells.

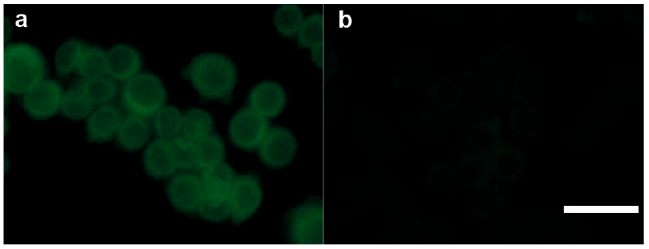

Figure 9. Epifluorescent microscopy of SK-BR-3 cells treated with **dPy-Tz-BODIPY**. (a) Prior to the treatment with the fluorophore, the cells were treated with nanobody 2RB17C-**caa-**$\mathbf{OBF_3}$. (b) Control experiment−nanobody treatment was omitted. Scale bar represents 40 μm. For better comparison and contrast, the pictures were thresholded from the original range 0−255 to 2−30.

CONCLUSIONS

In summary, potassium arylethynyltrifluoroborates were developed as a new class of dienophiles to react with tetrazines in a fast and controllable manner. This handle is reasonably small, easy to synthesize, and biocompatible. Both tetrazine and arylethynyltrifluoroborate handles were chemically in-

https://doi.org/10.1021/acs.bioconjchem.1c00276
Bioconjugate Chem. 2021, 32, 1812−1822

corporated onto proteins in a site-selective manner and labeled with complementary probes. The unique reactivity between arylethynyltrifluoroborates and pyridyl tetrazines allowed mutually orthogonal labeling by two IEDDA reactions. The combined advantages of temporal control over reactivity, stability, and orthogonality allow application of the arylethynyltrifluoroborate unstrained dienophile in mutually orthogonal protein labeling and construction of new biomaterials based simply on this $AlCl_3 \cdot 6H_2O$ triggered IEDDA ligation reaction.

■ ASSOCIATED CONTENT

Supporting Information

The Supporting Information is available free of charge at https://pubs.acs.org/doi/10.1021/acs.bioconjchem.1c00276.

Methods, supporting figures and tables, additional data, and characterization (PDF)

■ AUTHOR INFORMATION

Corresponding Authors

Gonçalo J. L. Bernardes − *Yusuf Hamied Department of Chemistry, University of Cambridge, CB2 1EW Cambridge, United Kingdom; Instituto de Medicina Molecular João Lobo Antunes, Faculdade de Medicina, Universidade de Lisboa, 1649−028 Lisboa, Portugal;* orcid.org/0000-0001-6594-8917; Email: gb453@cam.ac.uk

Gonzalo Jiménez-Osés − *Center for Cooperative Research in Biosciences (CIC bioGUNE), Basque Research and Technology Alliance (BRTA), 48160 Derio-Bizkaia, Spain; Ikerbasque, Basque Foundation for Science, 48009 Bilbao, Spain;* orcid.org/0000-0003-0105-4337; Email: gjoses@cicbiogune.es

Authors

Zbigniew Zawada − *Yusuf Hamied Department of Chemistry, University of Cambridge, CB2 1EW Cambridge, United Kingdom*

Zijian Guo − *Yusuf Hamied Department of Chemistry, University of Cambridge, CB2 1EW Cambridge, United Kingdom*

Bruno L. Oliveira − *Yusuf Hamied Department of Chemistry, University of Cambridge, CB2 1EW Cambridge, United Kingdom; Instituto de Medicina Molecular João Lobo Antunes, Faculdade de Medicina, Universidade de Lisboa, 1649−028 Lisboa, Portugal*

Claudio D. Navo − *Center for Cooperative Research in Biosciences (CIC bioGUNE), Basque Research and Technology Alliance (BRTA), 48160 Derio-Bizkaia, Spain;* orcid.org/0000-0003-0161-412X

He Li − *Yusuf Hamied Department of Chemistry, University of Cambridge, CB2 1EW Cambridge, United Kingdom*

Pedro M. S. D. Cal − *Instituto de Medicina Molecular João Lobo Antunes, Faculdade de Medicina, Universidade de Lisboa, 1649−028 Lisboa, Portugal*

Francisco Corzana − *Departamento de Química, Universidad de La Rioja, Centro de Investigación en Síntesis Química, 26006 Logroño, Spain;* orcid.org/0000-0001-5597-8127

Complete contact information is available at: https://pubs.acs.org/10.1021/acs.bioconjchem.1c00276

Author Contributions

[#]Z.Z. and Z.G. contributed equally.

Funding

We are grateful to the Czech Ministry of Education and ERDF/ESF (Postdoctoral fellowship to Z.Z. UOCHB MSCA Mobility II No. CZ.02.2.69/0.0/0.0/18_070/0010562), the China Scholarship Council (Ph.D. studentship to Z.G.), the Royal Society (URF to G.J.L.B., URF\R\180019), FCT Portugal (iFCT to G.J.L.B., IF/00624/2015; FCT Stimulus to P.M.S.DC. CEECIND/04518/2017 and to B.L.O., CEECIND/02335/2017), and Agencia Estatal de Investigación (Spain) (RTI2018−099592−B-C21 to F.C. and RTI2018−099592−B-C22 to G.J.O.) for funding. This project has received funding from the European Union's Horizon 2020 research and innovation program under Grant Agreement Nos. 676832, 702574, and 852985.

Notes

The authors declare no competing financial interest.

■ ACKNOWLEDGMENTS

Part of the computational resources were supplied by the project "e-Infrastruktura CZ" (e-INFRA LM2018140) provided within the program Projects of Large Research, Development and Innovations Infrastructures. The authors thank Dr. Vikki Cantrill for her help with the preparation and editing of this manuscript. Finally, we thank Dr. S. Massa and Prof. N. Devoogdt (Vrije Universiteit Brussel (VUM), Brussels) for the generous gift of the Her2-targeting nanobody 2Rb17c.

■ REFERENCES

(1) Carboni, R. A., and Lindsey, R. V. (1959) Reactions of Tetrazines with Unsaturated Compounds. A New Synthesis of Pyridazines. *J. Am. Chem. Soc. 81*, 4342−4346.

(2) Blackman, M. L., Royzen, M., and Fox, J. M. (2008) Tetrazine Ligation: Fast Bioconjugation Based on Inverse-Electron-Demand Diels-Alder Reactivity. *J. Am. Chem. Soc. 130*, 13518−13519.

(3) Darko, A., Wallace, S., Dmitrenko, O., Machovina, M. M., Mehl, R. A., Chin, J. W., and Fox, J. M. (2014) Conformationally strained trans-cyclooctene with improved stability and excellent reactivity in tetrazine ligation. *Chem. Sci. 5*, 3770−3776.

(4) Kozma, E., Nikić, I., Varga, B. R., Aramburu, I. V., Kang, J. H., Fackler, O. T., Lemke, E. A., and Kele, P. (2016) Hydrophilic trans-Cyclooctenylated Noncanonical Amino Acids for Fast Intracellular Protein Labeling. *ChemBioChem 17*, 1518−1524.

(5) Yang, J., Šečkute, J., Cole, C. M., and Devaraj, N. K. (2012) Live-Cell Imaging of Cyclopropene Tags with Fluorogenic Tetrazine Cycloadditions. *Angew. Chem., Int. Ed. 51*, 7476−7479.

(6) Ramil, C. P., Dong, M., An, P., Lewandowski, T. M., Yu, Z., Miller, L. J., and Lin, Q. (2017) Spirohexene-Tetrazine Ligation Enables Bioorthogonal Labeling of Class B G Protein-Coupled Receptors in Live Cells. *J. Am. Chem. Soc. 139*, 13376−13386.

(7) Devaraj, N. K., Weissleder, R., and Hilderbrand, S. A. (2008) Tetrazine-Based Cycloadditions: Application to Pretargeted Live Cell Imaging. *Bioconjugate Chem. 19*, 2297−2299.

(8) Deb, T., Tu, J., and Franzini, R. M. (2021) Mechanisms and Substituent Effects of Metal-Free Bioorthogonal Reactions. *Chem. Rev. 121*, 6850−6914.

(9) Lang, K., and Chin, J. W. (2014) Cellular incorporation of unnatural amino acids and bioorthogonal labeling of proteins. *Chem. Rev. 114*, 4764−4806.

(10) Rossin, R., van den Bosch, S. M., ten Hoeve, W., Carvelli, M., Versteegen, R. M., Lub, J., and Robillard, M. S. (2013) Highly Reactive trans-Cyclooctene Tags with Improved Stability for Diels-Alder Chemistry in Living Systems. *Bioconjugate Chem. 24*, 1210−1217.

(11) Niederwieser, A., Späte, A.-K., Nguyen, L. D., Jüngst, C., Reutter, W., and Wittmann, V. (2013) Two-Color Glycan Labeling of

Live Cells by a Combination of Diels-Alder and Click Chemistry. *Angew. Chem., Int. Ed. 52*, 4265−4268.
(12) Rieder, U., and Luedtke, N. W. (2014) Alkene-Tetrazine Ligation for Imaging Cellular DNA. *Angew. Chem., Int. Ed. 53*, 9168−9172.
(13) Shang, X., Song, X., Faller, C., Lai, R., Li, H., Cerny, R., Niu, W., and Guo, J. (2017) Fluorogenic protein labeling using a genetically encoded unstrained alkene. *Chem. Sci. 8*, 1141−1145.
(14) Oliveira, B. L., Guo, Z., Boutureira, O., Guerreiro, A., Jiménez-Osés, G., and Bernardes, G. J. L. (2016) A Minimal, Unstrained S-Allyl Handle for Pre-Targeting Diels-Alder Bioorthogonal Labeling in Live Cells. *Angew. Chem., Int. Ed. 55*, 14683−14687.
(15) Eising, S., Xin, B.-T., Kleinpenning, F., Heming, J. J. A., Florea, B. I., Overkleeft, H. S., and Bonger, K. M. (2018) Coordination-Assisted Bioorthogonal Chemistry: Orthogonal Tetrazine Ligation with Vinylboronic Acid and a Strained Alkene. *ChemBioChem 19*, 1648−1652.
(16) Eising, S., Engwerda, A. H. J., Riedijk, X., Bickelhaupt, F. M., and Bonger, K. M. (2018) Highly Stable and Selective Tetrazines for the Coordination-Assisted Bioorthogonal Ligation with Vinylboronic Acids. *Bioconjugate Chem. 29*, 3054−3059.
(17) Eising, S., Lelivelt, F., and Bonger, K. M. (2016) Vinylboronic Acids as Fast Reacting, Synthetically Accessible, and Stable Bioorthogonal Reactants in the Carboni-Lindsey Reaction. *Angew. Chem., Int. Ed. 55*, 12243−12247.
(18) Vivat, J. F., Adams, H., and Harrity, J. P. A. (2010) Ambient Temperature Nitrogen-Directed Difluoroalkynylborane Carboni-Lindsey Cycloaddition Reactions. *Org. Lett. 12*, 160−163.
(19) Molander, G. A., and Sandrock, D. L. (2009) Potassium trifluoroborate salts as convenient, stable reagents for difficult alkyl transfers. *Curr. Opin. Drug. Discovery Devel. 12*, 811−823.
(20) Darses, S., and Genet, J.-P. (2008) Potassium Organotrifluoroborates: New Perspectives in Organic Synthesis. *Chem. Rev. 108*, 288−325.
(21) Kirkham, J. D., Butlin, R. J., and Harrity, J. P. (2012) A mild benzannulation through directed cycloaddition reactions. *Angew. Chem., Int. Ed. 51*, 6402−6405.
(22) Bachollet, S. P., Vivat, J. F., Cocker, D. C., Adams, H., and Harrity, J. P. (2014) Development of a mild and versatile directed cycloaddition approach to pyridines. *Chem. - Eur. J. 20*, 12889−12893.
(23) Brown, A. W., Comas-Barceló, J., and Harrity, J. P. A. (2017) A Mild and Regiospecific Synthesis of Pyrazoleboranes. *Chem. - Eur. J. 23*, 5228−5231.
(24) Oliveira, B. L., Guo, Z., and Bernardes, G. J. L. (2017) Inverse electron demand Diels-Alder reactions in chemical biology. *Chem. Soc. Rev. 46*, 4895−4950.
(25) Lennox, A. J. J., and Lloyd-Jones, G. C. (2012) Organotrifluoroborate Hydrolysis: Boronic Acid Release Mechanism and an Acid-Base Paradox in Cross-Coupling. *J. Am. Chem. Soc. 134*, 7431−7441.
(26) Lang, K., Davis, L., Wallace, S., Mahesh, M., Cox, D. J., Blackman, M. L., Fox, J. M., and Chin, J. W. (2012) Genetic Encoding of Bicyclononynes and trans-Cyclooctenes for Site-Specific Protein Labeling in Vitro and in Live Mammalian Cells via Rapid Fluorogenic Diels-Alder Reactions. *J. Am. Chem. Soc. 134*, 10317−10320.
(27) Rideout, D. C., and Breslow, R. (1980) Hydrophobic acceleration of Diels-Alder reactions. *J. Am. Chem. Soc. 102* (26), 7816−7817.
(28) Knall, A.-C., Hollauf, M., and Slugovc, C. (2014) Kinetic studies of inverse electron demand Diels-Alder reactions (iEDDA) of norbornenes and 3,6-dipyridin-2-yl-1,2,4,5-tetrazine. *Tetrahedron Lett. 55*, 4763−4766.
(29) Lang, K., Davis, L., Torres-Kolbus, J., Chou, C., Deiters, A., and Chin, J. W. (2012) Genetically encoded norbornene directs site-specific cellular protein labelling via a rapid bioorthogonal reaction. *Nat. Chem. 4*, 298−304.
(30) Bernardim, B., Cal, P. M.S.D., Matos, M. J., Oliveira, B. L., Martinez-Saez, N., Albuquerque, I. S., Perkins, E., Corzana, F., Burtoloso, A. C.B., Jimenez-Oses, G., Bernardes, G. J. L., et al. (2016) Stoichiometric and irreversible cysteine-selective protein modification using carbonylacrylic reagents. *Nat. Commun. 7*, 13128.
(31) Bernardim, B., Matos, M. J., Ferhati, X., Compañón, I., Guerreiro, A., Akkapeddi, P., Burtoloso, A. C. B., Jiménez-Osés, G., Corzana, F., and Bernardes, G. J. L. (2019) Efficient and irreversible antibody-cysteine bioconjugation using carbonylacrylic reagents. *Nat. Protoc. 14*, 86−99.
(32) Lee, B., Sun, S., Jiménez-Moreno, E., Neves, A. A., and Bernardes, G. J. L. (2018) Site-selective installation of an electrophilic handle on proteins for bioconjugation. *Bioorg. Med. Chem. 26*, 3060−3064.
(33) Alam, I. S., Neves, A. A., Witney, T. H., Boren, J., and Brindle, K. M. (2010) Comparison of the C2A Domain of Synaptotagmin-I and Annexin-V As Probes for Detecting Cell Death. *Bioconjugate Chem. 21*, 884−891.
(34) Vaneycken, I., Devoogdt, N., Van Gassen, N., Vincke, C., Xavier, C., Wernery, U., Muyldermans, S., Lahoutte, T., and Caveliers, V. (2011) Preclinical screening of anti-HER2 nanobodies for molecular imaging of breast cancer. *FASEB J. 25*, 2433−2446.
(35) Yang, J., Liang, Y., Šečkute, J., Houk, K. N., and Devaraj, N. K. (2014) Synthesis and Reactivity Comparisons of 1-Methyl-3-Substituted Cyclopropene Mini-tags for Tetrazine Bioorthogonal Reactions. *Chem. - Eur. J. 20*, 3365−3375.
(36) Nikić, I., Plass, T., Schraidt, O., Szymański, J., Briggs, J. A. G., Schultz, C., and Lemke, E. A. (2014) Minimal Tags for Rapid Dual-Color Live-Cell Labeling and Super-Resolution Microscopy. *Angew. Chem., Int. Ed. 53*, 2245−2249.
(37) Nikić, I., Kang, J. H., Girona, G. E., Aramburu, I. V., and Lemke, E. A. (2015) Labeling proteins on live mammalian cells using click chemistry. *Nat. Protoc. 10*, 780.
(38) Kužmová, E., Zawada, Z., Navrátil, M., Günterová, J., and Kraus, T. (2021) Flow cytometric determination of cell cycle progression via direct labeling of replicated DNA. *Anal. Biochem. 614*, 114002.

https://doi.org/10.1021/acs.bioconjchem.1c00276
Bioconjugate Chem. 2021, 32, 1812−1822